Response-retaliation behaviour in synthetic protocell communities

Yan Qiao, Mei Li, Dong Qiu and Stephen Mann*

Prof. Dr. Y. Qiao, Dr. M. Li, Prof. Dr. S. Mann,

Centre for Protolife Research and Centre for Organized Matter Chemistry, School of Chemistry, University of Bristol, Bristol.

BS8 1TS, United Kingdom

E-mail: s.mann@bristol.ac.uk

Prof. Dr. Y. Qiao, Prof. Dr. D. Qiu,

Beijing National Laboratory for Molecular Sciences (BNLMS), State Key Laboratory of Polymer Physics and Chemistry, CAS Research/Education Center for Excellence in Molecular Sciences, Institute of Chemistry, Chinese Academy of Sciences, University of Chinese Academy of Sciences, Beijing 100190, China.

Supporting information for this article is given via a link at the end of the document.

Abstract

Two different artificial predation strategies are spatially and temporally coupled to generate a simple tit-for-tat mechanism in a ternary protocell network capable of antagonistic enzyme-mediated interactions. The consortium initially consists of protease-sensitive glucose oxidase-containing proteinosomes (**1**), non-interacting pH-sensitive polypeptide/mononucleotide coacervate droplets containing protease-K (**2**), and proteinosome-adhered pH-resistant polymer/polysaccharide coacervate droplets (**3**). On receiving a glucose signal, secretion of protons from **1** triggers the disassembly of **2** and the released protease is transferred to **3** to initiate a delayed contact-dependent killing of the proteinosomes and cessation of GOx activity. Our results provide a step towards complex mesoscale dynamics based on programmable response-retaliation behaviour in artificial protocell consortia.

Introduction

Dispersed communities of synthetic protocells based on mixed populations of lipid vesicles,[1,2] polymersomes,[3,4] colloidosomes,[5] proteinosomes,[6] and coacervate micro-droplets[7-9] provide an attractive opportunity to develop functionally interactive micro-compartmentalized systems capable of chemical communication,[10-17] sensing,[18] signal-induced differentiation,[19,20] distributed computing[21] oligonucleotide trafficking[22] and enzyme-powered buoyancy.[23] Increasing the complexity of these

consortia by exploiting matter and energy fluxes to drive cognate interactions remains a key challenge and a critical step towards synthetic protocell ecosystems exhibiting higher order contact-dependent behavior such as artificial phagocytosis[24,25] and prototissue assembly.[26,27]

We recently reported an experimental strategy for initiating artificial predatory behavior in a mixed dispersion of protein-polymer semi-permeable micro-capsules (proteinosomes) and polymer-nucleotide membrane-free coacervate micro-droplets loaded with a protease.[28] Electrostatically mediated contact-dependent interactions between the different protocell types gave rise to proteolytically induced disassembly of the individual proteinosomes and transfer of their macromolecular payloads into the predator coacervate droplets. Conversely, proteinosomes loaded with glucose oxidase (GOx) have been used to capture and disassemble pH-sensitive fatty acid coacervate droplets using an external β-D-glucose signal to programme the enzyme-mediated acidification of the binary population.[29] Herein, we couple these two artificial predation strategies to demonstrate a simple tit-for-tat mechanism in a mixed protocell community capable of antagonistic enzyme-mediated interactions. In so doing, our results provide a step towards more complex mesoscale dynamics based on programmable response-retaliation (tit-for-tat) behaviour in artificial protocell networks.

Results and Discussion

Experimental design and general strategy

Rudimentary tit-for-tat behaviour was achieved in a ternary protocell community using a consortium consisting of (**i**) a predatory population of large protease-sensitive GOx-containing proteinosomes capable of secreting a toxin (H^+) on receipt of a β-D-glucose signal, (**ii**) a population of small target protocells in the form of non-interacting pH-sensitive poly-D-lysine (PLys)/adenosine 5′-diphosphate (ADP) coacervate droplets containing sequestered protease-K as a latent antidote against proteinosome attack, and (**iii**) a counter-attacking population of proteinosome-adhered pH-resistant poly(diallyldimethylammonium chloride) (PDDA)/dextran-sulfate (DS) coacervate droplets that were initially dormant but became charged with protease by transfer and sequestration of the enzyme following proteinosome-induced disassembly of the PLys/ADP protocells (Figure 1a). To facilitate the response-retaliation process we used poly-D-lysine in place of poly-L-lysine to prevent protease-induced self-degradation of the target coacervate droplets, ADP rather than ATP to increase the pH sensitivity of the target protocells to attack by the GOx-containing proteinosomes, and PDDA/DS to protect the

counter-attacking protocells against proteinosome-induced acidification (Figure 1b-d). Moreover, we used coacervates prepared from PLys/ADP or PDDA/DS because they exhibited high equilibrium partition constants (K_P) for protease K (K_P = 300 and 200, respectively). This enabled high concentrations of the antidote to be housed in the target PLys/ADP droplets and provided an efficient mechanism for the transfer and re-capture of the protease payload by the counter-attacking PDDA/DS droplets. The surface charge of the coacervate droplets was modulated by use of appropriate stoichiometric ratios to produce negatively charged target PLys/ADP and positively charged killer PDDA/DS coacervate droplets (Figure 2a) that were considerably smaller (mean diameter, 2 and 0.5 μm, respectively) than the negatively charged proteinosomes (mean diameter, 20 μm) (Figures 2b,c). As a consequence, direct interactions between the proteinosomes and target PLys/ADP droplets were minimised in binary mixtures (Figure 2d), whilst the counter-attacking PDDA/DS droplets were adsorbed onto the outer surface of the proteinosome membrane (Figure 2e).

Antagonistic enzyme-mediated predation in proteinosome/coacervate protocell binary communities

Given the above considerations, we performed a series of initial experiments to establish the optimum conditions for attaining response-retaliation behavior in an interacting ternary protocell community comprising antagonistic pH- and protease-induced killing pathways. Addition of β-D-glucose (1 mM) to a binary population of GOx-containing proteinosomes and PLys/ADP droplets at a proteinosome : coacervate droplet number ratio of 1 : 100 resulted in a slow (buffered) decrease in the bulk pH from 7.5 to 5.5 within 35 min (Figure 3a). This was consistent with passive diffusion of β-glucose across the proteinosome membrane and triggering of GOx activity within the protocell interior to produce hydrogen peroxide and D-glucono-δ-lactone (GDL), followed by efflux of the low molecular weight products into the bulk solution and slow hydrolysis of GDL to D-gluconic acid. As a consequence, the high turbidity of the binary population remained initially unchanged for around 10 min after addition of glucose, after which the pH decreased below 7.0 and the optical transmittance increased up to a value of 100% at pH < 5.5 (Figure 3a). We attributed the increase in optical transmittance to disassembly of the coacervate phase by weakening of the polypeptide-nucleotide charge interactions due to progressive protonation of ADP associated with GOx activity within the proteinosome population. In contrast, minimal changes in pH and turbidity were observed for binary populations prepared in the absence of glucose or for mixtures of glucose and PLys/ADP droplets (Figure 3a).

Proteinosome-mediated depletion of the PLys/ADP coacervate population was confirmed visually by in situ optical and fluorescence microscopies (Figure 3b,c and Supporting Information, Figure S1 and

Movie S1) and statistically by fluorescence-activated cell sorting (FACS) using mixtures of DyLight 405-labelled proteinosomes (blue fluorescence) and FITC-PLys-doped PLys/ADP coacervate micro-droplets (green fluorescence) prepared at a proteinosome : coacervate micro-droplet number ratio of approximately 1 : 100 (volume ratio = 5 : 1). Significantly, whilst both protocell populations were resolved in the 2D pseudo-color plots obtained in the absence of glucose (Figure 3d-f), only GOx-containing proteinosomes remained at 60 min after addition of glucose (Figure 3g). Time-dependent FACS profiles recorded over a period of 14 min and initiated 20 min after addition of glucose indicated that obliteration of the coacervate population occurred relatively quickly, typically within 5 min, whilst the proteinosome count remained effectively unchanged (Figure 3h and Supporting Information Figure S2). In contrast, only minimal changes were observed in the time-dependent FACS profiles for control experiments involving binary populations of GOx-proteinosomes and PLys/ADP coacervate droplets prepared in the absence of glucose (Figure 3i and Supporting Information, Figure S3).

Having established the conditions for the glucose-triggered proteinosome-based predation of target PLys/ADP coacervate droplets, we sought to implement an appropriate tit-for-tat response by priming the negatively charged proteinosome membrane with positively charged PDDA/DS coacervate droplets (see Figure 2e), which were capable of acquiring proteolytic weaponry after disassembly of the PLys/ADP protocells. To assess the killing potential of the surface-adsorbed droplets, we labelled the proteinosomes using DyLight 405 (blue fluorescence) and PDDA/DS droplets with rhodamine isothiocyanate (RITC)-PDDA (red fluorescence), respectively, and exposed the mixed population to protease concentrations in free solution that were below the threshold required for proteinosome disassembly. Optical and fluorescence microscopy images showed coacervate-mediated disassembly of the proteinosomes for sequestered protease concentrations of ~3.5 μM (external concentration, ~17.5 nM) (Figure 3j,k), whilst partitioned concentrations of less than 1.0 μM (external concentration, 5 nM) had minimal killing potential (Supporting Information, Figure S4).

Tit-for-tat behavior in ternary protocell communities

Based on these observations, we prepared a ternary protocell community consisting of DyLight 405-labelled GOx-containing proteinosomes, protease K-loaded PLys/ADP coacervate droplets and PDDA/DS coacervate droplets at an approximate number ratio of 1 : 50 : 50. The protease was labelled with RITC (10%) to help determine the spatiotemporal positioning of the antidote during the experiments. To minimize cross-contamination arising from adventitious interactions between the proteinosomes and protease-containing PLys/ADP droplets, or between the two different types of oppositely charged

coacervate micro-droplets, we sedimented the latter onto glass slides and then gently added a pre-mixed dispersion of the GOx-containing proteinosomes and PDDA/DS droplets. Consistent with the above experiments on binary protocell populations, optical and fluorescence microscopy images recorded prior to the addition of glucose showed a predominance of PDDA/DS-coated proteinosomes along with unattached PDDA/DS and PLys/ADP coacervate droplets (Figure 4a). Addition of glucose gave rise to disassembly of a proportion of the target PLys/ADP droplets followed by destruction of the predatory proteinosomes within a period of 30-35 min (Figures 4b,c and Movie S2). Partial solubilization of the PLys/ADP droplets occurred rapidly over a period of ca. 1 min (Figure 4d) with concomitant loss of red fluorescence due to release of the sequestered protease (Figure 4e). In contrast, the PDDA/DS droplets remained unchanged in size and developed a red fluorescence (Figure 4d,e), indicating transfer and capture of the released RITC-protease. Taken together, the results indicated that the protease-based weaponry remained functional within the protocell network and that the anti-predation strategy was effective against the initial proteinosome-mediated acid attack.

Significantly, the level of reciprocity was dependent on the localized enrichment of protease K by the PDDA/DS coacervate droplets adsorbed at the surface of the proteinosomes. This was confirmed by control experiments performed using the same enzyme concentrations but involving a binary population of GOx-containing proteinosomes and protease-containing PLys/ADP droplets (Supporting Information, Figure S5). In this case, the PLys/ADP droplets were disassembled after addition of glucose but the proteinosomes remained intact, indicating that the concentration of protease K released into the bulk solution was insufficient to destabilize the protein-polymer membrane of the proteinosomes. Thus, the tit-for-tat behaviour was fundamentally dependent on the ability of the surface-absorbed PDDA/DS protocells to act as a micro-compartmentalized platform to enrich and relocate the released protease in close contact with the membrane of the predatory proteinosomes.

Conclusion

In conclusion, we have demonstrated a rudimentary response-retaliation pathway that provides a step towards programming the population dynamics of an interacting community of artificial cells. Controlling such behaviour through a single input signal requires the implementation and coupling of antagonistic interactions between different members of the consortium, and is facilitated by spatial positioning of the protocells, the dynamics of their internalized reactions, and efficiency of their chemical communication. Each of these criteria is compromised by noise in the system arising

principally from cross-contamination or short-circuiting of the network through adventitious proteolytic interactions between the protease-loaded PLys/ADP coacervate droplets and GOx-containing proteinosomes or extraneous transfer of protease K between the two different types of oppositely charged coacervate droplets. Whilst we were able to alleviate this by partially immobilizing the protease-containing PLys/ADP droplets on a substrate surface and maintaining a contact-dependent counter-attack, operating the network in stirred suspensions (as undertaken for FACS analysis for example) resulted in extensive depletion of the proteinosome population along with retention of the PLys/ADP droplets in the initial stages of the reaction cycle (Supporting Information, Figure S6). In principle, different levels of protocell survival should be attained by systematic changes in the relative number densities of the predatory proteinosomes, target PLys/ADP coacervate droplets and their killer PDDA/DS droplet counterparts. Studies on the detailed population dynamics in these protocell networks as well as the development of alternative approaches based on the spatial patterning and immobilization of the ternary community using acoustic standing waves[30] will be investigated in future work.

Acknowledgements

We thank the ERC Advanced Grant Scheme (No. 740235 (S.M.)), and Engineering and Physical Sciences Research Council, UK (EP/L002957/1) and BBSRC (BrisSynBio, Bristol Centre for Synthetic Biology; BB/L01386X/1) for financial support. We thank Dr Avinash Patil and Dr Jianbo Liu for fruitful discussions, Mr. Alan Leard and Dr. Katy Jepson for assistance with confocal microscopy, and Dr Andrew Herman and Lorena Sueiro Ballesteros for assistance with FACS.

Keywords: synthetic protocell • coacervate • proteinosome • response-retaliation behaviour • enzyme

References:

[1] E. Altamura, F. Milano, R. R. Tangorra, M. Trotta, O. H. Omar, P. Stano, F. Mavelli, *Proc. Natl. Acad. Sci. U. S. A.* 2017, *114*, 3837-3842.
[2] K. P. Adamala, A. E. Engelhart, J. W. Szostak, *Nat. Commun*. 2016, *7*, 11041.
[3] W. S. Jang, S. C. Park, E. H. Reed, K. P. Dooley, S. F. Wheeler, D. Lee, D. A. Hammer, *Soft Matter*. 2016, *12*, 1014-1020.
[4] H. Che, J. C. M van Hest, *J. Mater. Chem. B*. 2016, *4*, 4632-4647.
[5] M. Li, R. L. Harbron, J. V. M. Weaver, B. P. Binks, S. Mann*, Nat. Chem*. 2013, *5*, 529-536.
[6] X. Huang, M. Li, D. C. Green, D. S. Williams, A. J. Patil, S. Mann, *Nat. Commun*. 2013, *4*, 2239.
[7] S. Koga, D. S. Williams, A. W. Perriman, S. Mann, *Nat. Chem*. 2011, *3*, 720-724.
[8] B. Drobot, J. M. Iglesias-Artola, K. Le Vay, V. Mayr, M. Kar, M. Kreysing, H. Mutschler, T. D. Tang, *Nat. Commun*. 2018, *9*, 3643.
[9] R. R. Poudyal, R. M. Guth-Metzler, A. J. Veenis, E. A. Frankel, C. D. Keating, P. C. Bevilacqua, *Nat. Commun*. 2019, *10*, 490.
[10] P. M. Gardner, K. Winzer, B. G. Davis, *Nat. Chem*. 2009, *1*, 377-383.

[11] R. Lentini, S. P. Santero, F. Chizzolini, D. Cecchi, J. Fontana, M. Marchioretto, C. Del Bianco, J. L. Terrell, A. C. Spencer, L. Martini, M. Forlin, M. Assfalg, M. Dalla Serra, W. E. Bentley, S. S. Mansy, *Nat. Commun*. 2014, *5*, 4012.
[12] M. Weitz, J. Kim, K. Kapsner, E. Winfree, E. Franco, F.C. Simmel, *Nat. Chem*. 2014, *6*, 295-302.
[13] D. S. Williams, A. J. Patil, S. Mann, *Small*. 2014, *10*, 1830-1840.
[14] S. Sun, M. Li, F. Dong, S. Wang, L. Tian, S. Mann, *Small*. 2016, *12*, 1920-1927.
[15] M. Schwarz-Schilling, L. Aufinger, A. Muckl, F. C. Simmel, *Integr. Biol*. 2016, *8*, 564-570.
[16] K. P. Adamala, D. A. Martin-Alarcon, K. R. Guthrie-Honea, E. S. Boyden, *Nat. Chem*. 2017, *9*, 431-439.
[17] T-Y.D. Tang, D. Cecchi, G. Fracasso, D. Accardi, A. Coutable-Pennarun, S. S. Mansy, A. W. Perriman, J. L. R. Anderson, S. Mann, *ACS Synth. Bio*. 2018, *7*, 339-346.
[18] L. Tian, M. Li, J. Liu, A. J. Patil, B. W. Drinkwater, S. Mann, *ACS Cent. Sci*. 2018, *4*, 1551-1558.
[19] A. Dupin, F. C. Simmel, *Nat. Chem*. 2019, *11*, 32-39.
[20] L. Tian, M. Li, A. J. Patil, B. W. Drinkwater, S. Mann, *Nat. Commun.* 2019, *10***,** 3321.
[21] A. Joesaar, S. Yang, B. Bogels, A. van der Linden, P. Pieters, B. Kumar, N. Dalchau, A. Phillips, S. Mann, T. F. A. de Greef, *Nat. Nanotech*. 2019, *14*, 369-378.
[22] N. Martin, L. Tian, D. Spencer, A. Coutable-Pennarun, J. L. R. Anderson, S. Mann, *Angew. Chem. Int. Ed*. 2019, *58***,** 14594-14598.
[23] B. V. V. S. P. Kumar, A. J. Patil, S. Mann, *Nat. Chem*. 2018, *10*, 1154-1163.
[24] L. Rodríguez-Arco, M. Li, S. Mann, *Nat. Mater*. 2017, *16*, 857-863.
[25] L. Rodríguez-Arco, P. B. B. V. S Kumar, M. Li, A. J. Patil, S. Mann, *Angew. Chemie. Int. Ed.* 2019, *58*, 6333-6337.
[26] M. J. Booth, V. R. Schild, A. D. Graham, S. N. Olof, H. Bayley, *Sci. Adv*. 2016, *2*, e1600056.
[27] P. Gobbo, A. J. Patil, M. Li, R. Harniman, W. H. Briscoe, S. Mann, *Nat. Mater*. 2018, *17*, 1145-1153.
[28] Y. Qiao, M. Li, R. Booth, S. Mann, *Nat. Chem*. 2017, *9*, 110-119.
[29] N. Martin, J. P. Douliez, Y. Qiao, R. Booth, M. Li, S. Mann, *Nat. Commun*. 2018, *9*, 3652.
[30] L. Tian, N. Martin, P. G. Bassindale, A. J. Patil, M. Li, A. Barnes, B. W. Drinkwater, S. Mann. *Nat. Commun*. 2016, *7*, 13068.

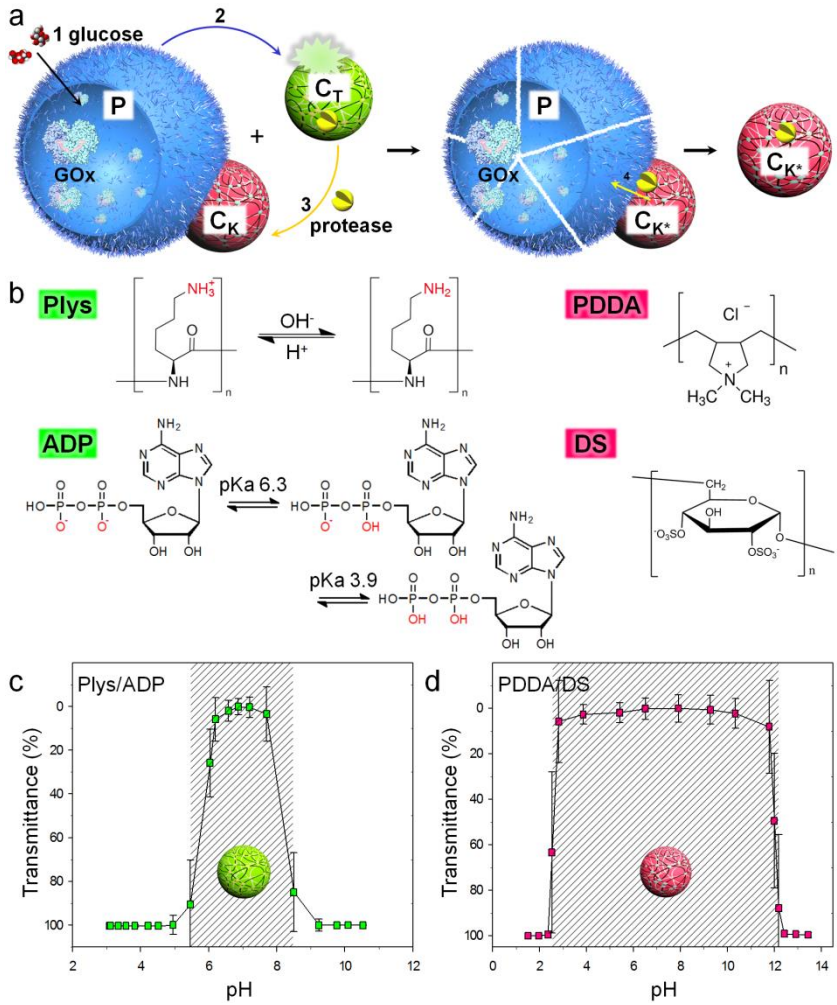

Figure 1. Response-retaliation behaviour in synthetic protocell communities. (**a**) Scheme showing general design of a rudimentary tit-for-tat behaviour in a consortium consisting of predatory protease-sensitive GOx-containing proteinosomes (**P**), pH-sensitive target PLys/ADP coacervate micro-droplets ($\mathbf{C_T}$) loaded with protease K (yellow notched object), and pH-insensitive counter-attacking killer PDDA/DS coacervate micro-droplets ($\mathbf{C_K}$). **P** and $\mathbf{C_T}$ are negatively charged and therefore non-interacting while **P** and $\mathbf{C_K}$ are physically in contact due to complementary surface potentials. A glucose input signal (**1**) gives rise to GOx-mediated secretion of H^+ ions (**2**) that disassembles $\mathbf{C_T}$ and releases protease, which is subsequently captured and re-concentrated by $\mathbf{C_K}$ (**3**). Given the close proximity of **P** and the protease-activated droplets ($\mathbf{C_{K*}}$), proteolytic digestion at the contact points results in P membrane disassembly (ruptured blue proteinosome) and dis-arming of the GOx payload (**4**). (**b**) Molecular structures and acid/base properties of PLys, ADP, PDDA and DS. (**c,d**) pH-dependent transmittance of PLys/ADP (**c**) and PDDA/DS (**d**) coacervate droplets. Hatched regions delineate the pH ranges associated with the formation of stable coacervate droplets. Experiments were undertaken at [PLys] = 1 mM, [ADP] = 1.3 mM; [PDDA] = 3.9 mM, [DS] = 3 mM.

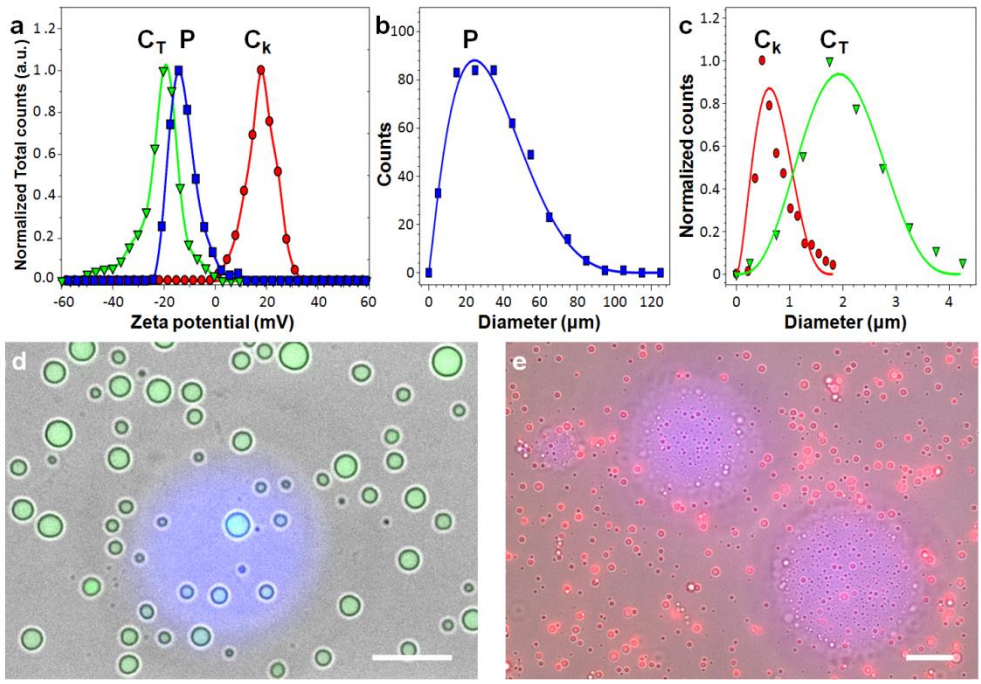

Figure 2. (**a**) Zeta potential distributions determined for aqueous suspensions of **P** (blue curve, -14 mV), as-prepared $\mathbf{C_T}$ (green curve, PLys/ADP monomer molar ratio = 1 : 1.3, - 20 mV) and $\mathbf{C_K}$ (red curve, PDDA/DS = 1.3 : 1, + 18 mV). (**b,c**) Size distributions of **P** (**b**), and $\mathbf{C_T}$ and $\mathbf{C_K}$ protocells (**c**). (**d**) Overlays of fluorescence and optical images showing a single DyLight 405-labelled GOx-containing proteinosome (blue fluorescence) and numerous non-interacting FITC-PLys-doped PLys/ADP coacervate micro-droplets (green fluorescence) recorded 6 h after mixing in the absence of glucose at pH 8.0; scale bar = 10 µm. (**e**) As for (**d**), but for mixtures of GOx-proteinosomes (blue fluorescence) and PDDA/DS coacervate droplets (red fluorescence) showing multiple coacervate droplets adsorbed onto the surface of the three proteinosomes along with non-attached PDDA/DS droplets. The image was recorded 6 h after mixing in the presence of glucose at pH < 5.5, confirming the pH stability of the PDDA/DS droplets in the presence of GOx-mediated acidification; scale bar = 10 µm.

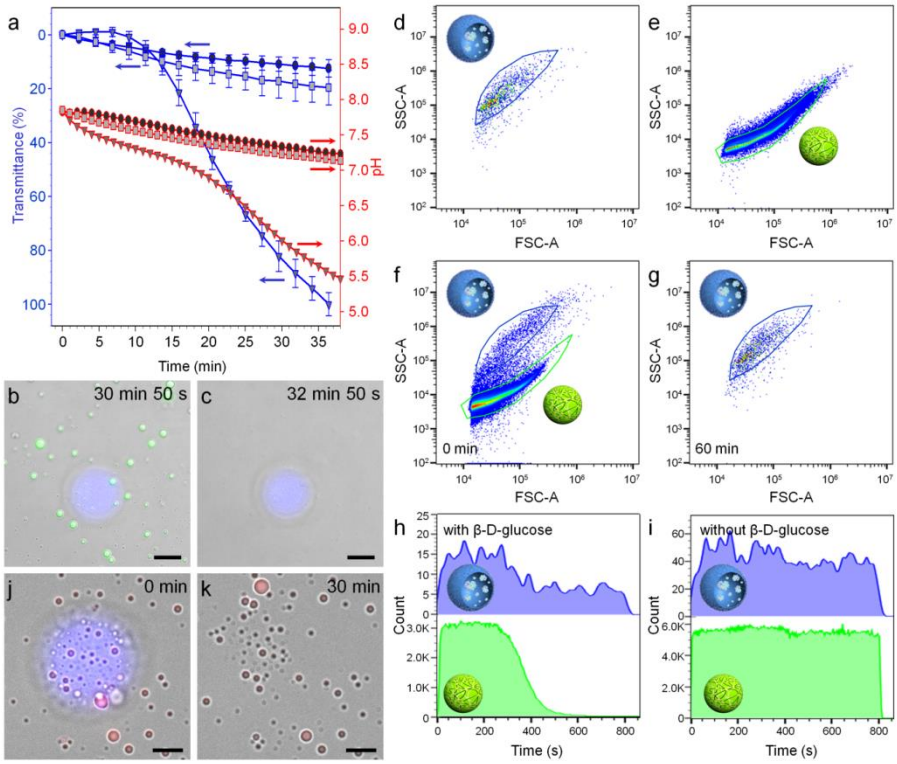

Figure 3. Population dynamics in binary protocell communities. (**a**) Overlay of plots showing time-dependent changes in pH (red curves) and optical transmittance (blue curves) for binary populations of GOx-containing proteinosomes (**P**) and target PLys/ADP coacervate micro-droplets ($\mathbf{C_T}$) in the presence of glucose (filled triangles, 1 mL of **P**, 200 µL of $\mathbf{C_T}$, [β-D-glucose] = 1 mM), mixtures of **P** and $\mathbf{C_T}$ without glucose (filled squares, 1 mL of **P**, 200 µL of $\mathbf{C_T}$) and mixtures of $\mathbf{C_T}$ with glucose (filled circles, 1 mL of H_2O, 200 µL of $\mathbf{C_T}$, [β-D-glucose] = 1 mM). (**b,c**) Overlaid optical and fluorescent microscopy images of a single DyLight 405-labelled GOx-containing proteinosome (blue fluorescence) in association with a population of FITC-PLys-doped PLys/ADP coacervate micro-droplets (green fluorescence) in the presence of glucose. The images in (**b**) and (**c**) were recorded ca. 30 min 50 s and 32 min 50 s after glucose addition, respectively, during which time the PLys/ADP droplets disassemble due to acidification; scale bars, 10 µm. (**d-g**) 2D pseudocolor FACS plots of forward-scattered (FSC) vs side-scattered (SSC) light for single populations of **P** (**d**) or $\mathbf{C_T}$ (**e**), binary **P** + $\mathbf{C_T}$ populations measured immediately after mixing and addition of glucose (t = 0 min) showing initial coexistence of proteinosomes (blue domain) and PLys/ADP coacervate micro-droplets (green domain) (**f**), and same sample as in **f** but 60 min after addition of glucose showing obliteration of the $\mathbf{C_T}$ population (**g**); ($\mathbf{P/C_T}$ number ratio = 1 : 100; n = 20,000; data recording time, 300 s). (**h,i**) Plots of time-dependent variation of particle counts over a period of 14 min for populations of **P** (blue) and $\mathbf{C_T}$ (green) recorded 20 min after mixing with (**h**) or without (**i**) glucose. Both plots show approximately constant counts for the proteinosome population. Random fluctuations in the number of particles detected by FACS are observed. In contrast, the coacervate population decreases to zero in the present of glucose (**h**) but not without glucose (**i**). Counts were determined from the corresponding 2D plots and were considerably lower for the proteinosome population. (**j,k**) Overlaid fluorescence and optical microscopy images of a single GOx-containing proteinosome (blue fluorescence) with surface-attached PDDA/DS coacervates ($\mathbf{C_K}$, red fluorescence) immediately (**j**) and 30 min (**k**) after addition of protease (3.5 µM of internal concentration and ~17.5 nM of external concentration) into a **P** + $\mathbf{C_k}$ suspension (**P** : $\mathbf{C_T}$ number ratio = 1 : 100), showing obliteration of the proteinosome; scale bars, 5 µm.

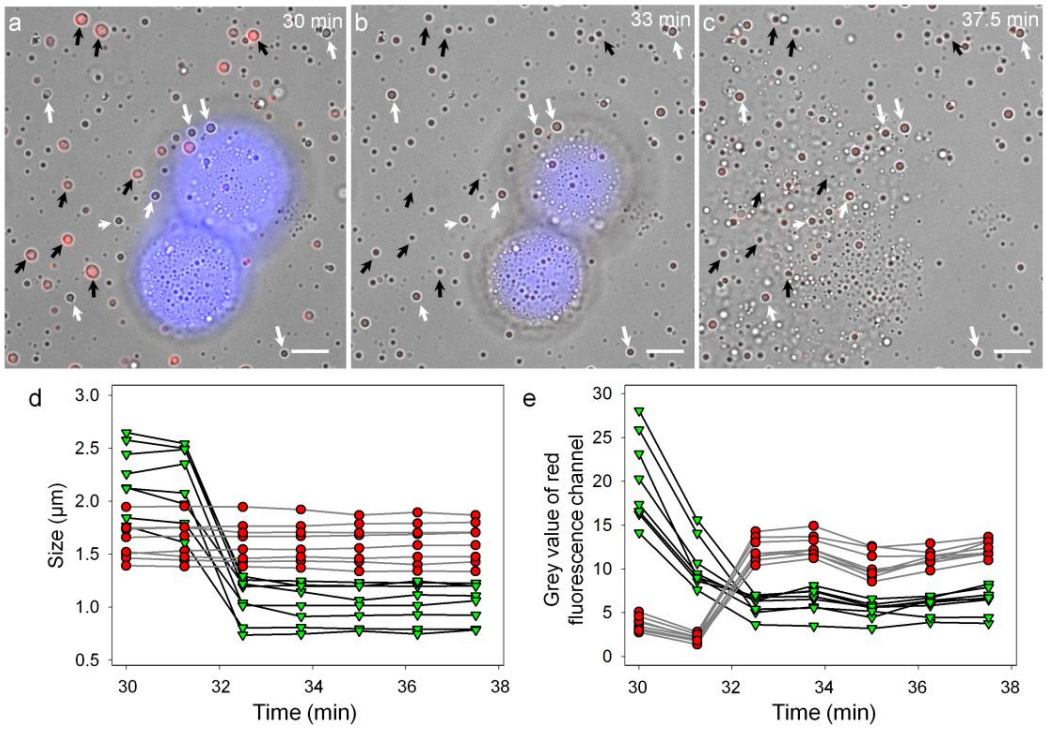

Figure 4. Tit-for-tat behaviour in ternary protocell communities. (**a-c**) Time sequence of overlaid fluorescence and optical microscopy images initially showing two GOx-containing proteinosomes (blue fluorescence), RITC-protease-loaded PLys/ADP coacervate droplets (black arrows, red fluorescence) and unlabelled PDDA/DS coacervate droplets (white arrows) recorded 30 (**a**), 33 (**b**) and 37.5 min (**c**) after addition of glucose. With time, the PLys/ADP droplets decrease in size and lose their red fluorescence while the PDDA/DS droplets remain constant in size and develop red fluorescence (**b**), followed by disassembly of the proteinosomes (**c**); scale bars, 10 µm. (**d,e**) Corresponding plots of time-dependent changes in coacervate droplet size (**d**) and coacervate-localized red fluorescence (**e**) for individual PLys/ADP (green triangles) and PDDA/DS (red circles) coacervate droplets identified by black and white arrows in **a-c**, respectively.

Table of Contents

Two artificial predation strategies are spatially and temporally coupled to generate rudimentary tit-for-tat behaviour in a ternary community of chemically interacting synthetic protocells.

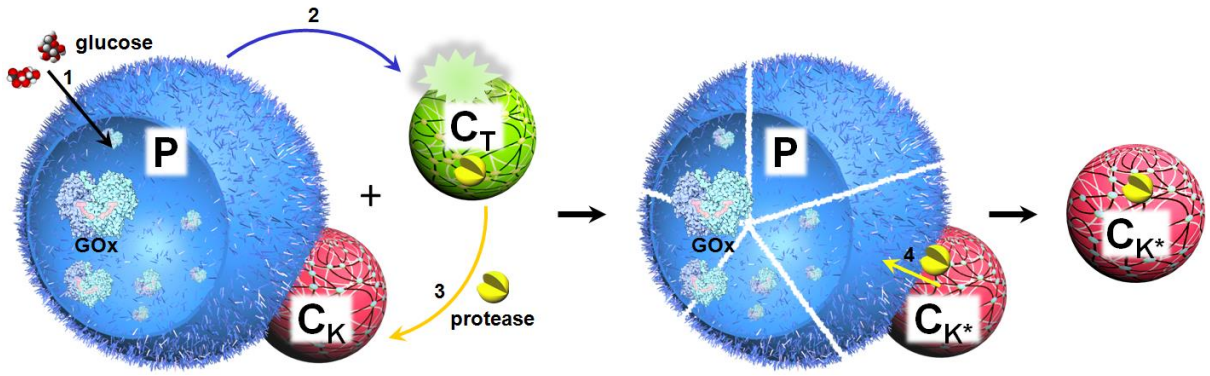

ChemDraw structures of Figure 1